

Received: 2019.07.01  
Accepted: 2019.09.20  
Published: 2019.10.07

# $C_{18}H_{17}NO_6$ Inhibits Invasion and Migration of Human MNNG Osteosarcoma Cells via the PI3K/AKT Signaling Pathway

Authors' Contribution:  
Study Design A  
Data Collection B  
Statistical Analysis C  
Data Interpretation D  
Manuscript Preparation E  
Literature Search F  
Funds Collection G

ABCDEF 1 **Qianqian Qu**  
BDE 2 **Zhongshun He**  
DE 1 **Yulei Jiang**  
AE 3 **Di Lu**  
BCD 4 **Xiaolin Long**  
EF 1 **Yu Ding**  
AFG 1 **Biao Xu**  
ADF 5 **Xiaoqiong He**

1 Stomatology Hospital Affiliated to Kunming Medical University, Kunming, Yunnan, P.R. China  
2 Yan'an Hospital Affiliated to Kunming Medical University, Kunming, Yunnan, P.R. China  
3 Biomedical Engineering Center of Kunming Medical University, Kunming, Yunnan, P.R. China  
4 Kunming Medical University, Kunming, Yunnan, P.R. China  
5 School of Public Health Kunming Medical University, Kunming, Yunnan, P.R. China

**Corresponding Authors:** Biao Xu, e-mail: xubiao1962@163.com, Xiaoqiong He, e-mail: hexqcn@aliyun.com  
**Source of support:** This study was funded by the Yunnan Science and Technology Department (2017FE468)

**Background:** Osteosarcoma (OS) is a highly aggressive, metastatic bone tumor with a poor prognosis, and occurs more commonly in children and adolescents. Therefore, new drugs and treatments are urgently needed. In this study, we investigated the effect and potential mechanisms of  $C_{18}H_{17}NO_6$  on osteosarcoma cells.

**Material/Methods:** Human MNNG osteosarcoma cells were treated with different concentrations of  $C_{18}H_{17}NO_6$ . The proliferation of the MNNG cells was examined via CCK-8 assay. Cell migration and invasion were tested via wound-healing assay and Transwell migration and invasion assays. ELISA was used to detect MMP-2, MMP-9, and VEGF secretion. Finally, Western blotting and qRT-PCR were used to detect protein and mRNA expressions, respectively.

**Results:**  $C_{18}H_{17}NO_6$  inhibited MNNG proliferation in a dose- and time-dependent manner and inhibited MMP-2, MMP-9, and VEGF secretion.  $C_{18}H_{17}NO_6$  treatment significantly downregulated N-cadherin and Vimentin expression levels and upregulated E-cadherin expression levels *in vitro* and *in vivo*.  $C_{18}H_{17}NO_6$  inhibited tumor growth in a MNNG xenograft. We also found that  $C_{18}H_{17}NO_6$  can significantly reduce the phosphorylation of the PI3K/AKT signaling pathway *in vivo* and *in vitro*. However, 740Y-P (a PI3K agonist) had the opposite effect on proliferation, migration and invasion of MNNG cells treated with  $C_{18}H_{17}NO_6$ . LY294002 (a PI3K inhibitor) downregulated p-PI3K and p-AKT could mimic the inhibitory effect of  $C_{18}H_{17}NO_6$ .

**Conclusions:** Our results suggest that  $C_{18}H_{17}NO_6$  can inhibit human MNNG osteosarcoma cell invasion and migration via the PI3K/AKT signaling pathway both *in vivo* and *in vitro*.  $C_{18}H_{17}NO_6$  may be a highly effective and low-toxicity natural drug for the prevention or treatment of OS.

**MeSH Keywords:** Cell Migration Assays • Medicine, Chinese Traditional • Neoplasm Invasiveness • Osteosarcoma

**Full-text PDF:** <https://www.medscimonit.com/abstract/index/idArt/918431>

 3519  1  4  30



## Background

Osteosarcoma (OS) is a primary malignant bone tumor most commonly found in children and adolescents [1]. In adolescent malignant tumors, the incidence of OS is second only to that of lymphoma, accounting for 3–4% of pediatric tumors and 30% of malignant bone tumors [2]. Although great progress has been made in treating OS, the recurrence and metastasis of this tumor remain uncontrolled, and the 5-year survival rate of patients with metastasis to the lungs is less than 20%. Postoperative recurrence and metastasis are also important factors affecting the prognosis of OS patients. To treat malignant bone tumors, planned comprehensive treatment is advocated, mainly with surgery supplemented by radiotherapy and chemotherapy [3]. However, these treatment methods cannot meet the needs of all patients and can cause additional harm to the body. It is urgent to develop new drugs with strong anticancer effect and low toxicity.

Traditional Chinese Medicine has been used to treat cancers for many years, with good therapeutic effects. However, basic research into its applications has just begun worldwide, and many problems remain unsolved. Traditional Chinese Medicine is reported to have achieved good results in treating liver cancer [4], lung cancer [5], gastric cancer [6], cervical cancer [7], glioma [8], osteosarcoma [9] and other cancers. C<sub>18</sub>H<sub>17</sub>NO<sub>6</sub> [6-acetyl-2-(1-amino-ethylidene)-7, 9-dihydroxy-8, 9b-dimethyl-9bH-dibenzofuran-1, 3-dione] is a new, natural anticancer drug with low toxicity extracted from a special plant *Usnea* in Yunnan, China. This drug significantly inhibits the proliferation of lung cancer, liver cancer, bladder cancer, breast cancer, and nasopharyngeal carcinoma cells, with IC<sub>50</sub> of 1.68, 1.91, 2.11, 2.51, and 3.39 μM, respectively. It can also induce apoptosis and cell cycle arrest in many types of cancer cells (patent ID: 201710388136.8). Notably, He et al. found that C<sub>18</sub>H<sub>17</sub>NO<sub>6</sub> combined with Scutellarin can inhibit proliferation and induce apoptosis of human glioma cells by upregulating Fas-Associated Factor 1 expression [10]. At present, there has been no relevant study on the effect of C<sub>18</sub>H<sub>17</sub>NO<sub>6</sub> on osteosarcoma cells. However, whether C<sub>18</sub>H<sub>17</sub>NO<sub>6</sub> can inhibit osteosarcoma cell proliferation, migration, and invasion and the specific mechanisms involved remain unclear and require further study.

The phosphatidylinositol 3-kinase/protein kinase B signaling pathway (PI3K/AKT) plays an important role in many cellular functions, including proliferation, adhesion, migration, invasion, metabolism, and survival. AKT has been reported to be over-activated in >60% of cancer types [11]. It is involved in tumor development and is also a potential target for tumor therapy. However, its role in C<sub>18</sub>H<sub>17</sub>NO<sub>6</sub>-inhibited osteosarcoma cell proliferation, migration, and invasion is still unclear.

We selected human MNNG osteosarcoma cells and treated them with different concentrations of C<sub>18</sub>H<sub>17</sub>NO<sub>6</sub> and established a MNNG xenograft model to examine the effects of C<sub>18</sub>H<sub>17</sub>NO<sub>6</sub> on human osteosarcoma cell proliferation, migration, and invasion, as well as the possible molecular mechanisms, *in vitro* and *in vivo*. This will provide an important theoretical basis for determining the experimental safety and efficacy of C<sub>18</sub>H<sub>17</sub>NO<sub>6</sub> *in vivo* and in clinical experiments.

## Material and Methods

### Cell lines and culture conditions

Human osteosarcoma cells (MNNG) were acquired from the Institute of Zoology, Chinese Academy of Sciences. MNNG cells were cultured at 37°C in Dulbecco's modified Eagle's medium (DMEM; HyClone, USA) supplemented with 10% fetal bovine serum (FBS; Gibco, USA) and 1% penicillin-streptomycin (HyClone, USA) in a cell incubator containing 5% CO<sub>2</sub>. When the cells grew to 80–90% confluence, digestion was terminated with 0.25% trypsin (HyClone, USA) after 2 min. After centrifugation at 600 rpm for 5 min, the cells were collected and subcultured according to experimental protocols.

### Cell counting kit-8 (CCK-8) detection

One hundred microliters of MNNG cell suspension in the logarithmic growth stage were inoculated into a 96-well plate with 5000 cells/well. Each group had 5 compound holes and were cultured at 37°C in 5% CO<sub>2</sub>. After 24 h of adherence, the cells were incubated with different concentrations of C<sub>18</sub>H<sub>17</sub>NO<sub>6</sub> for 24 h, 48 h, and 72 h. CCK-8 (DOJINDO, Japan) detection reagent (10 μl) was added to each well, and the absorbance (OD value) was measured at 450 nm after incubating for 2 h in an incubator. The inhibitory rate and survival rate were calculated as follows: inhibitory rate=(Ac-As)/(Ac-Ab)×100%; survival rate=1-inhibitory rate.

### Wound-healing assay

Three microliters of MNNG cell suspension in the logarithmic growth phase were inoculated into 6-well plates with approximately 1×10<sup>6</sup> cells/well and grown overnight. After discarding the supernatant, 5 horizontal lines were drawn on the bottom of the 6-hole plate with a marking pen. A 100-μl pipette tip was used to make 3 scratches evenly perpendicular to the marking line, which were then washed with 0.01 M phosphate-buffered saline (PBS) 3 times to remove the separated cells. The drug was diluted with DMEM and cultured at 37°C in 5% CO<sub>2</sub>. Ten images were taken at the same position under an inverted microscope at 0 h, 12 h, and 24 h (×40). Image J software was used to measure the area at 0 h, 12 h,

and 24 h. Mobility was calculated as (mean area at 0 h–mean area at x h)/(mean area at 0 h)×100%.

#### Transwell migration and invasion assays

Cell invasion was evaluated using serum-free medium and BD Matrigel diluted at 4: 1, then mixed, and kept on ice. After adding 100 µl diluted matrix glue to the upper chamber (Costar, 3422, USA) and incubating at 37°C for 2 h, a white membrane was visible to the naked eye. Matrigel was washed once with serum-free medium. After 48 h of drug treatment per group, the MNNG cells were collected to prepare the cell suspension, and 100 µl of the cell suspension was added to the upper chamber at 1×10<sup>4</sup> cells/well, and 500 µl complete culture medium containing 10% FBS was added to the lower chamber. The cells were incubated in a cell incubator for 48 h. Cells were removed from the upper chamber by wiping the surface with a cotton swab. Cells that had migrated to the membrane surface were fixed with 4% polyformaldehyde for 10 min, stained with 1% crystal violet (Leagene, China) for 10 min, and rinsed with 0.01 M PBS 3 times. Using a microscope, 5 visual fields (×200) were randomly selected to observe and count the cells.

To evaluate the cell migration, all the above steps were repeated but without adding BD Matrigel to the upper chamber.

#### Western blotting

MNNG cells were treated with C<sub>18</sub>H<sub>17</sub>NO<sub>6</sub> at different concentrations for 48 h, then the total protein was extracted via radioimmunoprecipitation assay buffer (Thermo Fisher Scientific, Inc.) (Solarbio, USA) adding 1% PMSF (Solarbio, USA) on ice. The protein concentration was determined using a bicinchoninic acid assay (Beyotime, China). The protein samples were transferred to a PVDF membrane (Millipore, MA, USA) after electrophoresis, then sealed at room temperature for 1 h with 5% skimmed milk, and dissolved in 1×TBST. Anti-MMP-2 (1: 2000; Abcam, ab97779), anti-MMP-9 (1: 1500; Abcam, ab58803), anti-E-cadherin (1: 1000; CST, 14472), anti-N-cadherin (1: 1000; CST, 14215), anti-Vimentin (1: 1000; CST, 5741), anti-PI3K (1: 1000; CST, 4292), anti-AKT (1: 5000; Abcam, ab179463), anti-p-PI3K (1: 1000; CST, 4228) and anti-p-AKT (1: 750; Abcam, ab38449) were incubated overnight at 4°C, then washed 3 times with 1×TBST for 10 min. The samples were incubated with corresponding secondary antibody diluted at 1: 5000 at room temperature for 1 h, then washed 3 times with 1×TBST for 10 min each time. Enhanced chemiluminescence detection reagent (MILLIPORE, USA) was used to develop the image. The ChemiDoc XSR+imaging system (BIO-RAD) was used for imaging. Image J software was used to analyze the gray-scale level. The average intensity ratio of the target protein to the internal reference was used for semiquantitative analysis of the target proteins.

**Table 1.** Primer sequences used for qRT-PCR analysis.

Genes	Primer sequence
MMP-2	Forward 5'-GAGTGCATGAACCAACCAGC-3'
	Reverse 5'-AAACTGCGAGGCTGCCTT-3'
MMP-9	Forward 5'-TCTATGGTCTCGCCCTGAA-3'
	Reverse 5'-TTGTATCCGGCAAAGTGGCT-3'
VEGF	Forward 5'-ACTTTGGTATCGTGAAGGACTCAT-3'
	Reverse 5'-GTTTTCTAGACGGCAGGTCAGG-3'

#### Quantitative real-time PCR (qRT-PCR)

Primers were designed according to the relevant target gene sequences published by GenBank. Table 1 lists the primers used for the qRT-PCR. Takara Biotechnology Co. synthesized the primers. After the MNNG cells were treated with C<sub>18</sub>H<sub>17</sub>NO<sub>6</sub> at different concentrations for 48 h, the total RNA was extracted according to the instructions of the Takara RNA extraction kit (Takara, Japan, 9767). The extracted total RNA was immediately re-transcribed into cDNA (Takara, Japan, RR047A). Finally, the fluorescence quantitative PCR reaction (Takara, Japan, RR820A) was carried out in an ABI7300 fluorescence quantitative PCR instrument. The thermocycling conditions were 95°C for 10 min, followed by 40 cycles of 95°C for 10 s and 60°C for 30 s. Expression of selected genes was normalized to GAPDH using the 2<sup>-ΔΔCT</sup> method.

#### Enzyme-linked immunosorbent assay (ELISA)

MNNG cells were treated with different concentrations of C<sub>18</sub>H<sub>17</sub>NO<sub>6</sub> for 48 h, then the conditioned medium was collected. The supernatant was centrifuged at a low temperature at 12 000 rpm for 15 min, and the supernatant was collected and stored at –80°C. The operation was performed according to the instructions provided with the ELISA kit. The matrix metalloproteinase-2 (MMP-2, Huamei, China, CSB-E04675h), matrix metalloproteinase-9 (MMP-9, Huamei, China, CSB-E08006h), and vascular endothelial growth factor (VEGF, Huamei, China, CSB-E11718h) secretion levels in each treatment group were detected.

#### Establishment of the MNNG xenograft model

Twelve female BALB/c-nu/nu mice weighing 18–22 g were randomly divided into the control and experimental groups, with 6 mice per group. MNNG cell suspensions were taken during the logarithmic growth stage. The cell concentration was adjusted to 5×10<sup>6</sup> cells/ml, and 0.2 ml MNNG cell suspension was subcutaneously injected into the right armpits of the mice. When the tumor volumes reached 180–200 mm<sup>3</sup>, the mice were randomly divided into the control or experimental group.

The experimental group was injected with 2 mg/kg C<sub>18</sub>H<sub>17</sub>NO<sub>6</sub>, i.p. qd; the control group was injected 0.9% physiological saline at the same dose and mode. The body weight, length and diameter of the tumor of the mice were recorded every 3 days. MNNG xenograft tumors were resected on day 20. Tumor volume was calculated as  $1/2a^2b$ , where “a” is the short diameter of the tumor, and “b” is the long diameter.

### Statistical analysis

Data are expressed as mean±SD of 3 independent experiments. Data analysis was done using the *t* test and one-way ANOVA. GraphPad prism 6 software was used for data analysis and mapping. Statistical significance was defined as  $p < 0.05$ .

## Results

### Effects of C<sub>18</sub>H<sub>17</sub>NO<sub>6</sub> on proliferation, migration, and invasion of MNNG cells

The inhibitory effect of C<sub>18</sub>H<sub>17</sub>NO<sub>6</sub> on MNNG cells was detected via CCK-8 and was found to occur in a time- and dose-dependent manner (Figure 1A). We measured the viability of MNNG cells treated with 0–100 μM C<sub>18</sub>H<sub>17</sub>NO<sub>6</sub> for 24 h, 48 h, and 72 h, and the IC<sub>50</sub>s (drug concentrations at a 50% inhibitory rate) of the MNNG cells were  $9.96 \pm 0.45$  μM,  $3.12 \pm 0.05$  μM, and  $2.13 \pm 0.04$  μM, respectively (Figure 1B). The cell viability decreased as the drug concentration increased ( $p < 0.01$ ). Thus, C<sub>18</sub>H<sub>17</sub>NO<sub>6</sub> inhibited MNNG cells in a time- and dose-dependent manner. We selected 3 concentrations (1.5 μM, 3 μM, and 4 μM) as the follow-up experimental concentrations.

We hypothesized that C<sub>18</sub>H<sub>17</sub>NO<sub>6</sub> could inhibit MNNG cell migration and invasion. The wound-healing assay showed that compared with the group at 12 h, the control group and the 1.5 μM C<sub>18</sub>H<sub>17</sub>NO<sub>6</sub> group showed migration ( $p < 0.05$ ) at 24 h, but the migration rates of the 3 μM and 4 μM C<sub>18</sub>H<sub>17</sub>NO<sub>6</sub> groups showed almost no differences at 24 h and were time- and dose-dependent (Figure 1C, 1D).

The Transwell invasion assay showed that the invasion ability in the C<sub>18</sub>H<sub>17</sub>NO<sub>6</sub>-treatment group was significantly lower than that of the control group ( $p < 0.01$ ) and was dose-dependent (Figure 1E, 1F). The Transwell migration assay showed that the migration ability of the C<sub>18</sub>H<sub>17</sub>NO<sub>6</sub> treatment group was significantly lower than that of the control group ( $p < 0.01$ ) and was dose-dependent (Figure 1E, 1G).

### Effects of C<sub>18</sub>H<sub>17</sub>NO<sub>6</sub> on MMPs and VEGF expression, EMT process, and PI3K/AKT signaling pathway

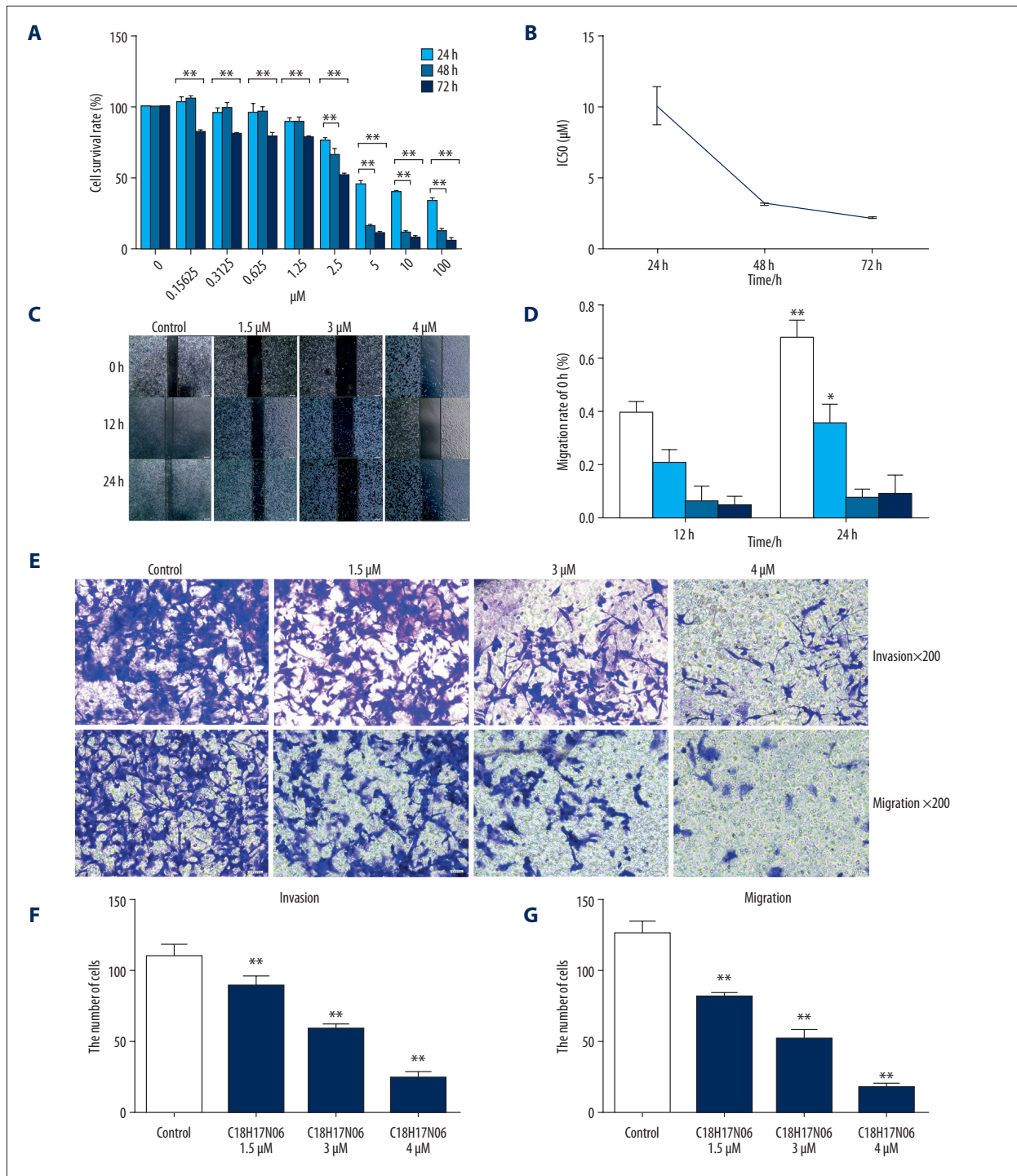
To further investigate the mechanism by which C<sub>18</sub>H<sub>17</sub>NO<sub>6</sub> inhibited MNNG cell migration and invasion, we assessed whether C<sub>18</sub>H<sub>17</sub>NO<sub>6</sub> affected MMP-2, MMP-9, and VEGF expression and secretion. Western blot results showed that the protein expression levels of MMP-2 and MMP-9 decreased as the C<sub>18</sub>H<sub>17</sub>NO<sub>6</sub> concentration increased. Among these, the 4 μM C<sub>18</sub>H<sub>17</sub>NO<sub>6</sub> group was significantly decreased ( $p < 0.01$ ; Figure 2A, 2B). qRT-PCR results showed that the mRNA expression levels of MMP-2 and MMP-9 decreased as the C<sub>18</sub>H<sub>17</sub>NO<sub>6</sub> concentration increased, among which the 4 μM C<sub>18</sub>H<sub>17</sub>NO<sub>6</sub> group decreased significantly ( $p < 0.01$ ; Figure 2C–2E). ELISA results showed that C<sub>18</sub>H<sub>17</sub>NO<sub>6</sub> reduced MMP-2 secretion in MNNG cells, and the 4 μM C<sub>18</sub>H<sub>17</sub>NO<sub>6</sub> group concentration was significantly reduced compared with that of the control group ( $p < 0.01$ ). C<sub>18</sub>H<sub>17</sub>NO<sub>6</sub> also reduced MMP-9 secretion from MNNG cells compared with that of the control group, with the 3 μM and 4 μM C<sub>18</sub>H<sub>17</sub>NO<sub>6</sub> groups showing significant decreases ( $p < 0.05$ ). C<sub>18</sub>H<sub>17</sub>NO<sub>6</sub> reduced VEGF secretion in MNNG cells compared with that of the control group, with the 3 μM and 4 μM C<sub>18</sub>H<sub>17</sub>NO<sub>6</sub> groups showing significant decreases ( $p < 0.05$ ) (Figure 2F–2H).

Epithelial-to-mesenchymal transition (EMT) plays an important role in tumor metastasis, and we hypothesized that C<sub>18</sub>H<sub>17</sub>NO<sub>6</sub> can affect the EMT process. Western blot results showed that as the C<sub>18</sub>H<sub>17</sub>NO<sub>6</sub> concentration increased and the N-cadherin and Vimentin expression levels decreased significantly ( $p < 0.01$ ), while the E-cadherin expression level increased significantly ( $p < 0.01$ ; Figure 2A, 2B).

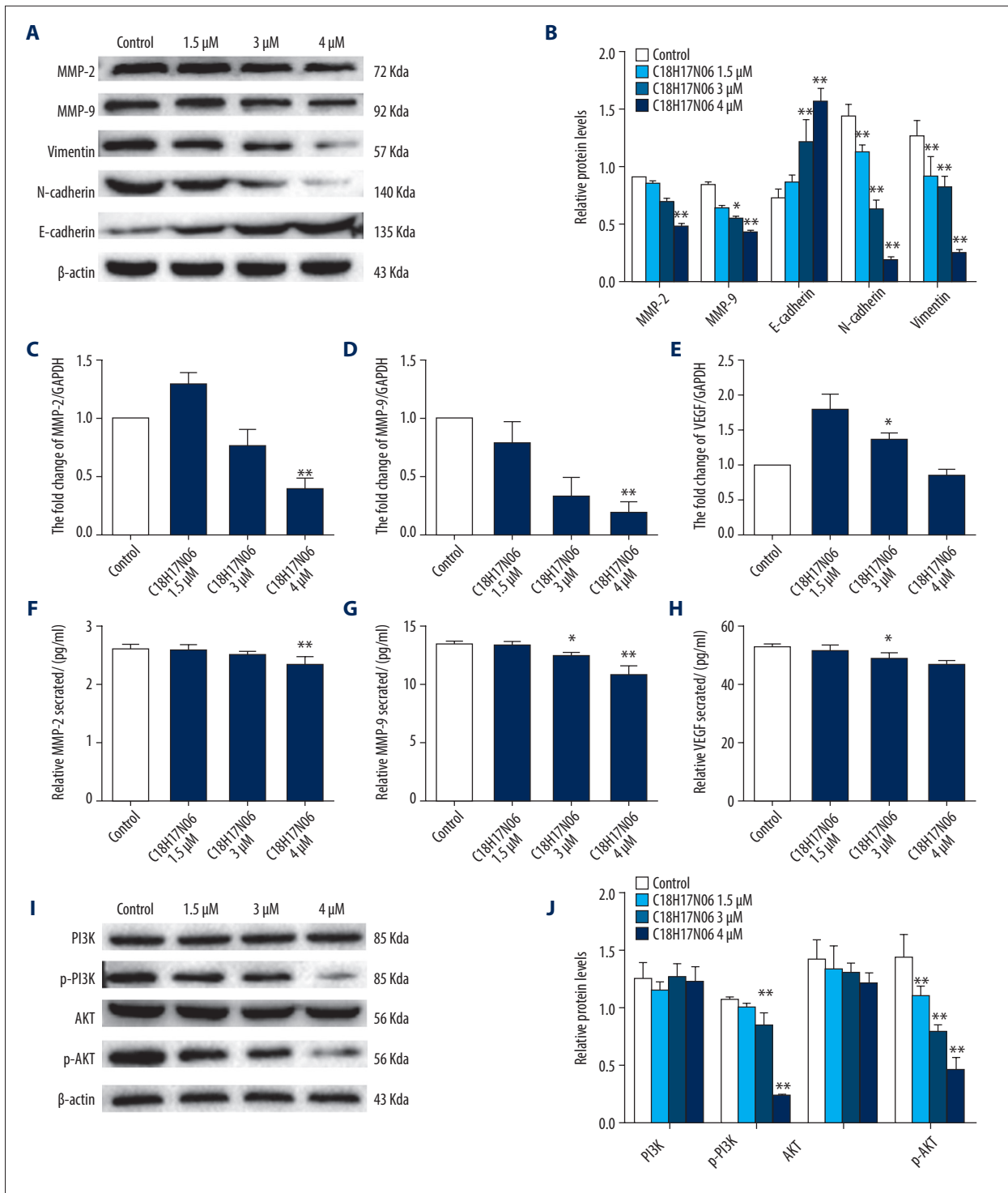
We hypothesized that C<sub>18</sub>H<sub>17</sub>NO<sub>6</sub> regulates the biological behavior of MNNG cells through the PI3K/AKT signaling pathway. We detected the protein expression changes of PI3K, p-PI3K, AKT, and p-AKT after MNNG cells were treated with different concentrations of C<sub>18</sub>H<sub>17</sub>NO<sub>6</sub> for 48 h. There was no significant change in total PI3K or total AKT. p-PI3K and p-AKT expression levels were dose-dependently decreased compared with those of the control group, especially in the 3 μM and 4 μM C<sub>18</sub>H<sub>17</sub>NO<sub>6</sub> groups ( $p < 0.01$ ; Figure 2I, 2J). We selected a concentration of 4 μM C<sub>18</sub>H<sub>17</sub>NO<sub>6</sub> as the follow-up experimental concentration.

### C<sub>18</sub>H<sub>17</sub>NO<sub>6</sub> suppresses proliferation, migration and invasion by inhibiting PI3K/AKT signaling pathway in MNNG cells

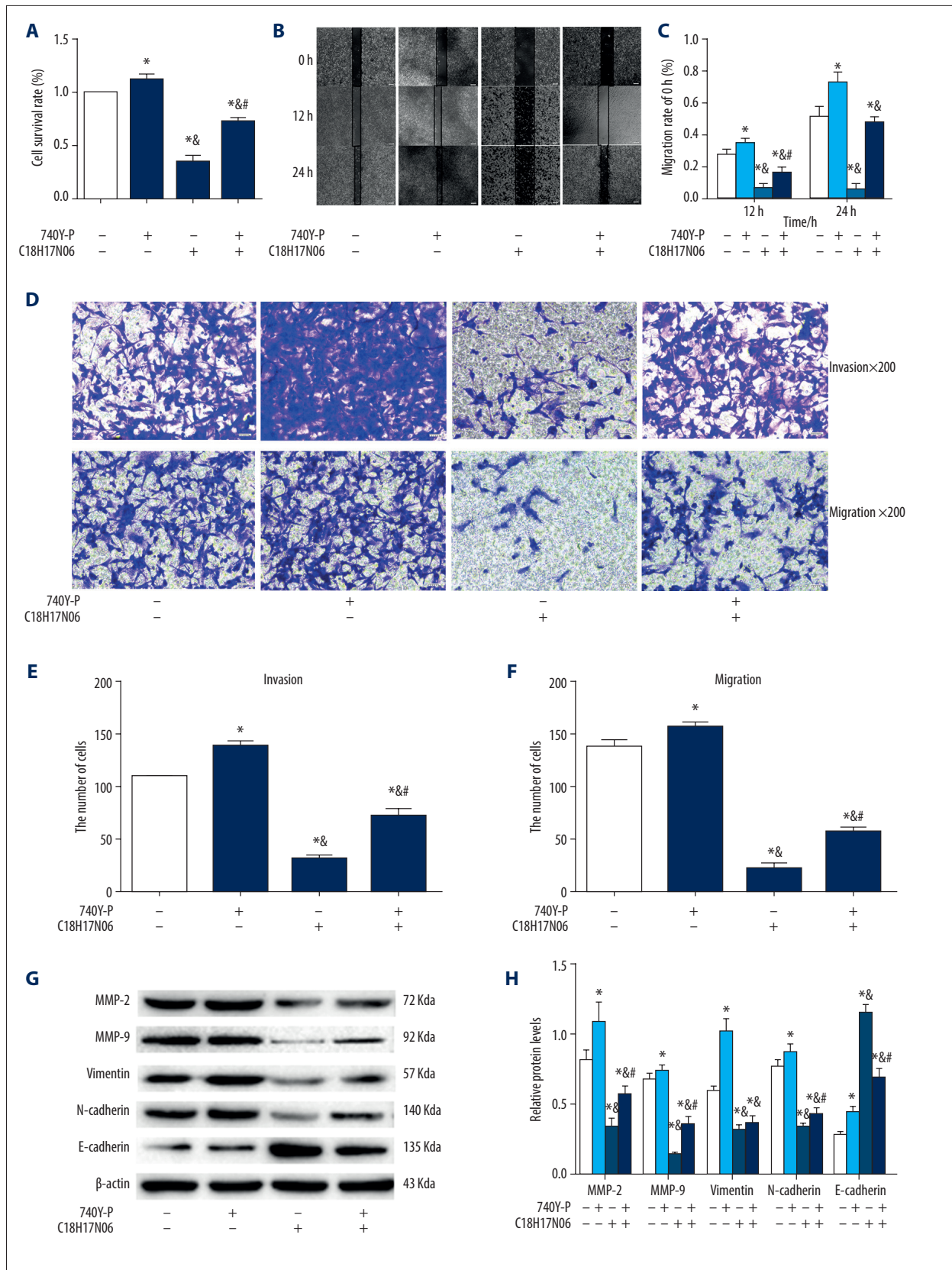
To confirm the results, 740Y-P (a PI3K agonist, Selleck, USA, S7865) and LY294002 (a PI3K inhibitor, Selleck, USA, S1105) were used to treat MNNG cells alone or combined with C<sub>18</sub>H<sub>17</sub>NO<sub>6</sub> for 48 h. Firstly, we found that 740Y-P at 20 μM remarkably increased the proliferation (Figure 3A), migration, and invasion (Figure 3B–3F) ability of MNNG cells ( $p < 0.05$ ), but these were significantly inhibited in the 4 μM



**Figure 1.** Effects of  $C_{18}H_{17}NO_6$  on MNNG cell proliferation, migration, and invasion. **(A)** Inhibitory effects of different concentrations of  $C_{18}H_{17}NO_6$  on MNNG cells. **(B)** The IC50 broken-line diagram of different concentrations of  $C_{18}H_{17}NO_6$  acting on the MNNG cells after 2 h, 4 h, and 72 h. **(C)** Pictures of different concentrations of  $C_{18}H_{17}NO_6$  acting on MNNG cell scratches after 12 h and 24 h ( $\times 40$ ) and quantitatively analyzed **(D)**. Data are expressed as mean $\pm$ SD of 3 independent experiments. Compared with 12h, \*  $p < 0.05$ , \*\*  $p < 0.01$ . The effects of different concentrations of  $C_{18}H_{17}NO_6$  on invasion of MNNG cells ( $\times 200$ ) **(E)** and quantitatively analyzed **(F)**. The effects of different concentrations of  $C_{18}H_{17}NO_6$  on the migration of MNNG cells ( $\times 200$ ) **(E)** and quantitatively analyzed **(G)**. Data are expressed as mean $\pm$ SD of 3 independent experiments. Compared with the control group, \*  $P < 0.05$ , \*\*  $P < 0.01$ .



**Figure 2.** The effects of different concentrations of  $C_{18}H_{17}NO_6$  on the MMPs, EMT process, and PI3K/AKT signaling pathway in MNNG cells. (A) Western blot analysis of MMP-2, MMP-9, N-cadherin, Vimentin, and E-cadherin in MNNG cells treated with different concentrations of  $C_{18}H_{17}NO_6$  for 48 h and quantitatively analyzed (B). qRT-PCR analysis of MMP-2 (C), MMP-9 (D), and VEGF (E) mRNA in MNNG cells treated with different concentrations of  $C_{18}H_{17}NO_6$  for 48 h. ELISA was used to detect the secretion levels of MMP-2 (F), MMP-9 (G), and VEGF (H). (I) Western blot analysis of PI3K, AKT, p-PI3K, and p-AKT after MNNG cells treated with different concentrations of  $C_{18}H_{17}NO_6$  for 48 h and quantitatively analyzed (J). Data are expressed as mean $\pm$ SD of 3 independent experiments. Compared with the control group, \*  $p < 0.05$ , \*\*  $p < 0.01$ .



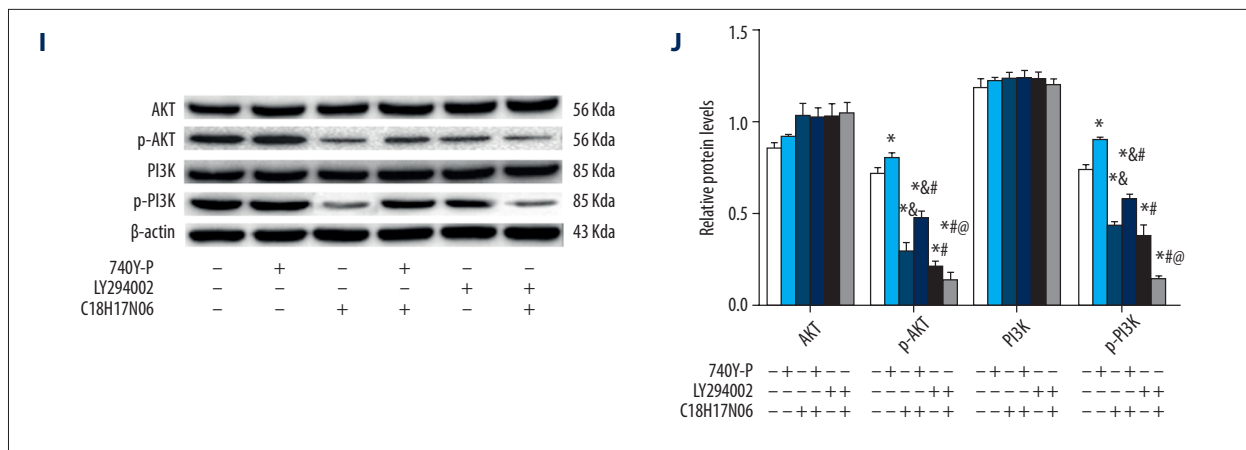


**Figure 3.** The effect of 740 Y-P (a PI3K activator) and LY294002 (a PI3K inhibitor) alone or combined with C<sub>18</sub>H<sub>17</sub>NO<sub>6</sub> on MNNG cells. (A) The effect of 740 Y-P and C<sub>18</sub>H<sub>17</sub>NO<sub>6</sub> or co-incubation on MNNG cell proliferation. (B) Images of 740 Y-P and C<sub>18</sub>H<sub>17</sub>NO<sub>6</sub> or co-incubation act on MNNG cell scratches after 12 h, 24 h (×40) and quantitatively analyzed (C). (D) The effects of 740 Y-P and C<sub>18</sub>H<sub>17</sub>NO<sub>6</sub> or co-incubation on invasion of MNNG cells (×200), quantitative analyzed (E). (F) The effects of 740 Y-P and C<sub>18</sub>H<sub>17</sub>NO<sub>6</sub> or co-incubation on the migration of MNNG cells (×200) (D) and quantitative analysis (F). (G) Western blot analysis of MMP-2, MMP-9, N-cadherin, Vimentin, and E-cadherin in MNNG cells treated with 740 Y-P and C<sub>18</sub>H<sub>17</sub>NO<sub>6</sub> or co-incubation for 48 h and quantitatively analyzed (H). (I) Western blot analysis of PI3K, AKT, p-PI3K, and p-AKT after MNNG cells treated with 740 Y-P and C<sub>18</sub>H<sub>17</sub>NO<sub>6</sub> or co-incubation for 48 h and quantitatively analyzed (J). Data are expressed as mean±SD of 3 independent experiments. Compared with the control group, \* p<0.05; Compared with the 740 Y-P group, & p<0.05; Compared with the C<sub>18</sub>H<sub>17</sub>NO<sub>6</sub> group, # p<0.05; Compared with the LY 294002 group, @ p<0.05.

C<sub>18</sub>H<sub>17</sub>NO<sub>6</sub> group (p<0.05). After co-incubation with 740Y-P, these changes were markedly rescued (p<0.05). Secondly, the protein expression levels of MMP-2, MMP-9, E-cadherin, N-cadherin, and Vimentin were evaluated. As shown in Figures 3G and 3H, the protein expression levels of MMP-2, MMP-9, N-cadherin, and Vimentin were significantly downregulated following treatment with 4 μM C<sub>18</sub>H<sub>17</sub>NO<sub>6</sub> (p<0.05). 740Y-P at 20 μM remarkably rescued this decrease (p<0.05). We obtained the opposite results in the protein expression levels of E-cadherin. Finally, to investigate whether the PI3K/AKT pathway participates in the inhibitory effect of C<sub>18</sub>H<sub>17</sub>NO<sub>6</sub> on MNNG cells, the cells were incubated with 740Y-P (20 μM), LY294002 (20 μM) alone, or in combination with C<sub>18</sub>H<sub>17</sub>NO<sub>6</sub> (4 μM) for 48 h. Compared to the control group, 740Y-P at 20 μM remarkably upregulated the protein expression of p-PI3K and p-AKT (p<0.05), and C<sub>18</sub>H<sub>17</sub>NO<sub>6</sub> at 4 μM and LY294002 at 20 μM treatment resulted in remarkably downregulated the protein expression of p-PI3K and p-AKT (p<0.05). After co-incubation with 740Y-P, C<sub>18</sub>H<sub>17</sub>NO<sub>6</sub>-dependent inhibition of the PI3K/AKT signaling pathway was eliminated. Co-incubation with LY294002 enhanced suppression of the PI3K/AKT signaling pathway (Figures 3I, 3J). These data at least partially suggest that C<sub>18</sub>H<sub>17</sub>NO<sub>6</sub> weakens MNNG cell proliferation, migration, and invasion by inhibiting the PI3K/AKT signaling pathway.

### Therapeutic effects of C<sub>18</sub>H<sub>17</sub>NO<sub>6</sub> on MNNG xenograft *in vivo*

The effect of C<sub>18</sub>H<sub>17</sub>NO<sub>6</sub> on OS *in vivo* was determined via MNNG xenograft in nude mice. The time-volume curve showed that the tumor volume of the C<sub>18</sub>H<sub>17</sub>NO<sub>6</sub> group decreased significantly (p<0.01; Figure 4A, 4B) compared with that of the control group. Furthermore, the PI3K, AKT, N-cadherin, E-cadherin, and Vimentin levels were detected via Western blot in the tumor tissues of each group. The results showed that p-PI3K and p-AKT, N-cadherin, and Vimentin expression levels in the C<sub>18</sub>H<sub>17</sub>NO<sub>6</sub> group were significantly decreased compared with the control group, while the E-cadherin expression level increased significantly (p<0.01; Figure 4C–4F). Thus, C<sub>18</sub>H<sub>17</sub>NO<sub>6</sub> inhibits the growth of MNNG xenograft and affects the EMT process and the PI3K/AKT signaling pathway *in vivo*.

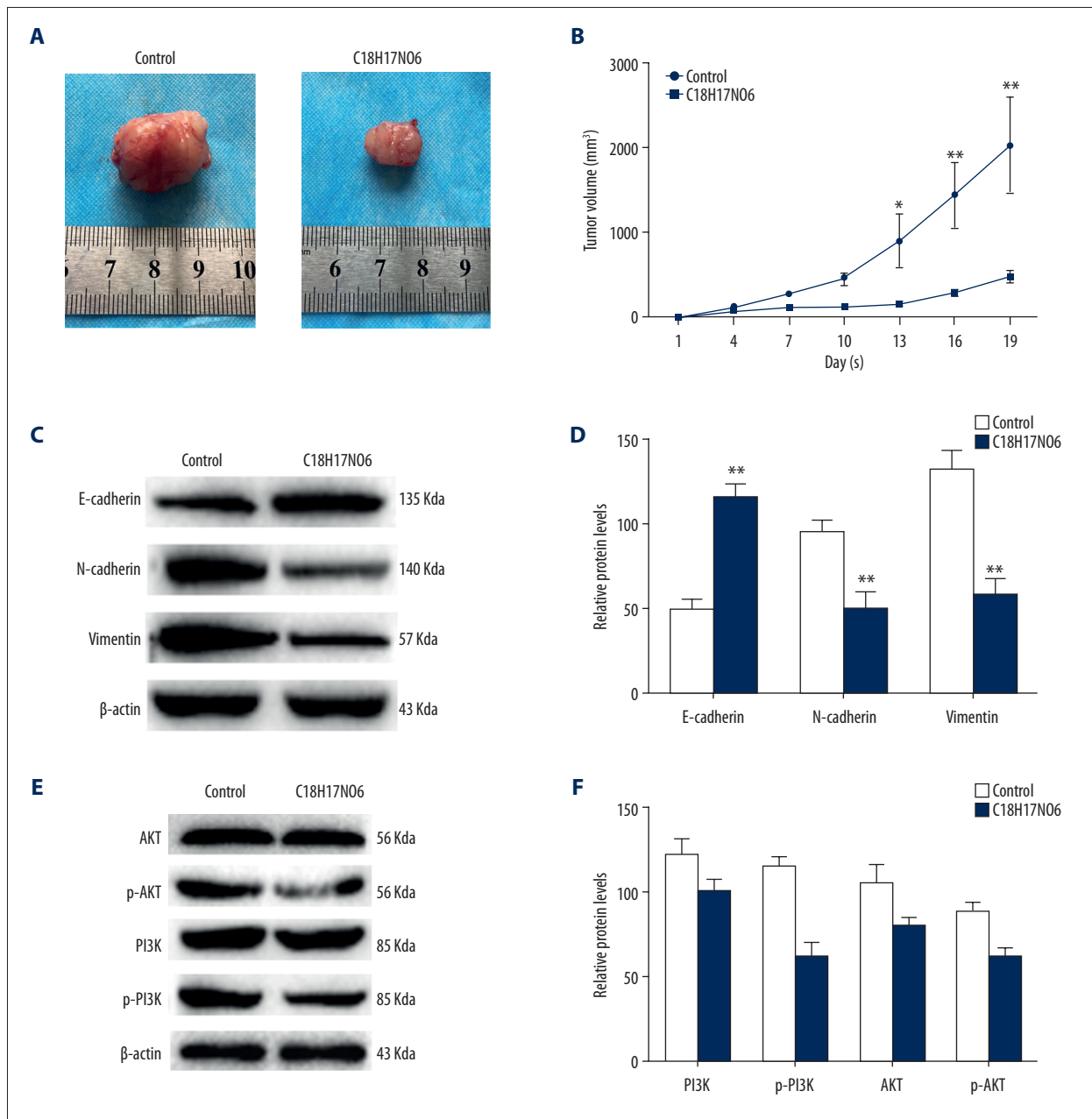
### Discussion

OS is the most common type of malignant primary bone tumor in children [12]. Advances in chemotherapy and surgical treatments have improved the 5-year survival rates of patients with OS. However, the 5-year survival rate of patients with pulmonary metastatic OS remains less than 20% due to its highly invasive metastatic potential and therapeutic resistance [13]. Therefore, new drugs and treatments are urgently needed.

$C_{18}H_{17}NO_6$  is a dibenzofuran compound extracted from a plant in Yunnan, China. It is a new, natural anticancer drug with low toxicity (patent ID: 201710388136.8). The purity of this compound can reach 99.5%. In this study, we obtained similar results for osteosarcoma cells to those of other tumor cells reported by Xiaoqiong He. Therefore,  $C_{18}H_{17}NO_6$  is a promising new drug for treating OS.

Metastasis, a major cause of cancer-related deaths, is a multi-step process involving local adhesion, migration, invasion, and degradation of the extracellular matrix and basement membrane with multiple proteases such as matrix metalloproteinases

(MMPs) and urokinase [14,15]. Because OS is characterized by high invasion and metastasis, the migration and invasion of MMNG cells after exposure to  $C_{18}H_{17}NO_6$  must be determined. MMPs plays an important role in cell metastasis [16]. MMP-2 and MMP-9 promote tumor metastasis and extracellular matrix (ECM) degradation [17]. We found that cell migration and invasion in the  $C_{18}H_{17}NO_6$ -treated group was significantly lower than that in the control group.  $C_{18}H_{17}NO_6$  reduced endogenous MMP-2 and MMP-9 expression and functional MMP-2 and MMP-9 secretion. Therefore, MMP-2 and MMP-9 may be the mediators of degradation of ECM by  $C_{18}H_{17}NO_6$ , which promotes the metastasis of osteosarcoma cells. Metastasis also



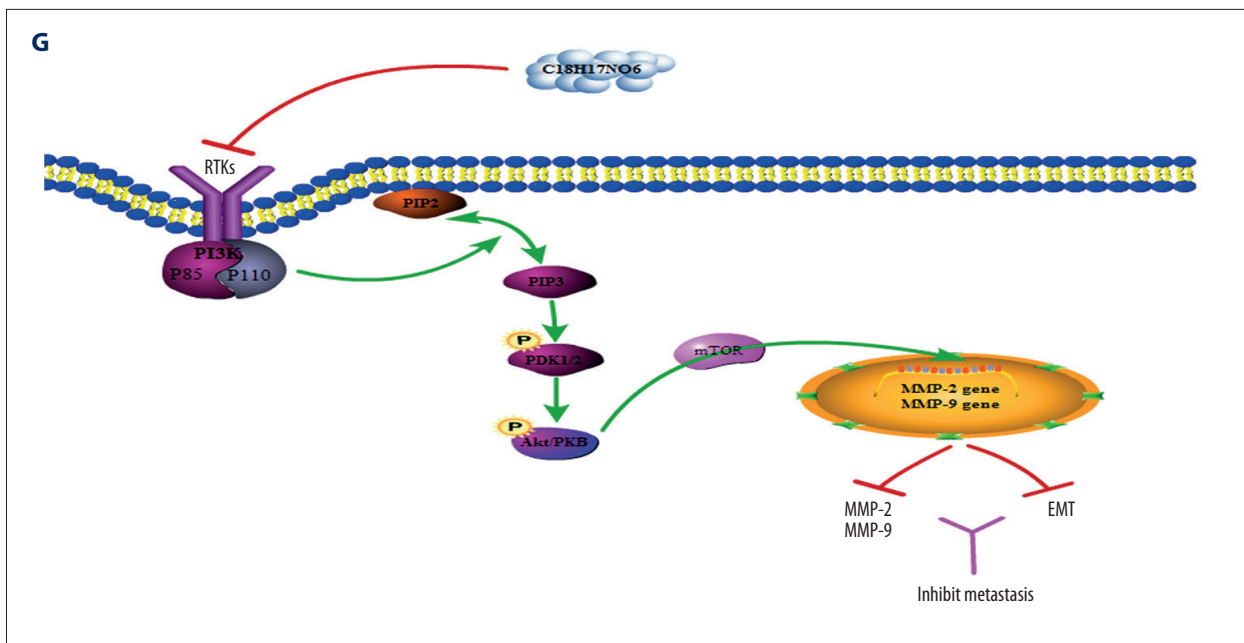


**Figure 4.** The anti-tumor effect of *C*<sub>18</sub>H<sub>17</sub>NO<sub>6</sub> on the BALB/c-nu mice bearing MNNG xenograft. (A) Images of tumors in the control group and *C*<sub>18</sub>H<sub>17</sub>NO<sub>6</sub>-treatment group. (B) The tumor volume at the indicated days was measured. (C, D) Western blot analysis of E-cadherin, N-cadherin, and Vimentin in the tumor tissues isolated from mice. (E, F) Western blot analysis of PI3K, AKT, p-PI3K, and p-AKT in the tumor tissues isolated from mice. (G) Schematic diagram of the signaling pathway of *C*<sub>18</sub>H<sub>17</sub>NO<sub>6</sub> inhibiting MNNG cell migration and invasion. Compared with the control group, \* *p*<0.05, \*\* *p*<0.01.

requires tumor cells to transition from the epithelium to a mesenchymal state and acquire the potential for migration [18]. The EMT is the early stage of solid tumor progression and is closely related to tumor growth, invasion, metastasis, and drug resistance and is conducive to the transformation of tumors from low-grade to high-grade malignancy [19,20]. It is reported that resveratrol inhibits migration and metastasis of human breast cancer cells by reversing the epithelial-mesenchymal transition [21]. In particular, EMT is reported to be a key event in OS metastasis [22] and many studies have demonstrated that upregulated expression of MMP-2 and MMP-9 contributes to EMT [23]. The deletion of E-cadherin can activate EMT, while the inhibition of MMP-9 is related to the renewal of E-cadherin [24]. Growth factors can induce morphological changes in cells, such as a loss of epithelial marker expression and increased mesenchymal marker expression [25], which are characteristics of the EMT. Among them, VEGF can be used as a prognostic biomarker for OS patients [26]. Finally, our study found that *C*<sub>18</sub>H<sub>17</sub>NO<sub>6</sub> treatment upregulated E-cadherin expression and inhibited VEGF secretion of MNNG cells. Taken together, our results show that using MMPs to restore or block downregulation of E-cadherin may be an effective strategy to control tumor metastasis and EMT progression.

The PI3K/AKT pathway is interrelated with many intracellular signaling pathways, thus participating in regulating a variety of cellular events, such as cell cycle progression and cell

proliferation, angiogenesis, invasion, and metastasis [27]. Previous studies have shown that PI3K/AKT/mTOR mediates the EMT and AKT can regulate the expression of MMP-related protein and cancer cell metastasis [16,28]. In our study, *C*<sub>18</sub>H<sub>17</sub>NO<sub>6</sub> inhibited migration and invasion in MNNG cells, suggesting that *C*<sub>18</sub>H<sub>17</sub>NO<sub>6</sub> regulates MNNG cell behavior through the PI3K/AKT signaling pathway. We found that *C*<sub>18</sub>H<sub>17</sub>NO<sub>6</sub> markedly inhibits the PI3K/AKT signaling pathway both *in vivo* and *in vitro*. Our results agree with the finding that Phellamurin inhibits osteosarcoma cell proliferation and migration via PI3K/Akt/mTOR signaling pathways [29]. Li et al. [30] reached the same conclusion after investigating the mechanism of Acledinium in osteosarcoma cells. To further confirm the role of the PI3K/AKT signaling pathway in inhibiting MNNG cell proliferation, migration, and invasion of *C*<sub>18</sub>H<sub>17</sub>NO<sub>6</sub>, we used 740Y-P (a PI3K agonist) and LY294002 (a PI3K inhibitor). We found that proliferation, migration, and invasion of MNNG cells were remarkably inhibited in the *C*<sub>18</sub>H<sub>17</sub>NO<sub>6</sub> treatment group but were increased in the *C*<sub>18</sub>H<sub>17</sub>NO<sub>6</sub>+740Y-P group, as evidenced by wound-healing assay, Transwell invasion and migration assays, higher protein expressions of MMP-2, MMP-9, N-cadherin, and Vimentin and lower protein expressions of E-cadherin. These results suggest that activation of the PI3K/AKT signaling pathway by 740Y-P can rescue the inhibitory effects of *C*<sub>18</sub>H<sub>17</sub>NO<sub>6</sub> on MNNG cells. The PI3K/AKT signaling pathway might be critical for *C*<sub>18</sub>H<sub>17</sub>NO<sub>6</sub>-mediated EMT and metastasis. In addition, LY294002-downregulated p-PI3K and p-AKT can mimic the

inhibitory effect of C<sub>18</sub>H<sub>17</sub>NO<sub>6</sub> on MNNG cells. In summary, all these results indicate that inhibition of the PI3K/AKT signaling pathway may have an important role in the proliferation, migration, and invasion of MNNG cells after C<sub>18</sub>H<sub>17</sub>NO<sub>6</sub> treatment (Figure 4G). Further studies are needed to investigate the effects of C<sub>18</sub>H<sub>17</sub>NO<sub>6</sub> in other types of osteosarcoma cells.

## Conclusions

In summary, C<sub>18</sub>H<sub>17</sub>NO<sub>6</sub> significantly inhibited MNNG cell proliferation, migration, and invasion, and this process may be related to inhibition of the PI3K/AKT signaling pathway. As a natural drug with strong anticancer properties, C<sub>18</sub>H<sub>17</sub>NO<sub>6</sub> is a

potential new anticancer drug for the treatment of OS invasion and metastasis.

## Acknowledgements

C<sub>18</sub>H<sub>17</sub>NO<sub>6</sub> was provided by Xiaoqiong He, School of Public Health, Kunming Medical University.

Equipment was provided by the Biomedical Engineering Center of Kunming Medical University.

## Conflict of interest

None.

## References:

- Xing XW, Sun YF, Zhao J et al: Tizanidine hydrochloride exhibits a cytotoxic effect on osteosarcoma cells through the PI3K/AKT signaling pathway. *J Int Med Res*, 2019; 47(8): 3792–802
- Wang W, Zhao HF, Yao TF, Gong H: Advanced development of ErbB family-targeted therapies in osteosarcoma treatment. *Invest New Drugs*, 2019; 37(1): 175–83
- Zohreh JA, Mohammad JA, Ali AA: Overexpression of CDC7 in malignant salivary gland tumors correlates with tumor differentiation. *Braz J Otorhinolaryngol*, 2019; 85(2): 144–49
- Ling CQ, Fan J, Lin HS et al: Clinical practice guidelines for the treatment of primary liver cancer with integrative traditional Chinese and Western medicine. *J Integr Med*, 2018; 16(4): 236–48
- Liu J, Lin HS, Hou W: Comprehensive treatment with Chinese medicine in patients with advanced non-small cell lung cancer: A multicenter, prospective, cohort study. *Chin J Integr Med*, 2017; 23(10): 733–39
- Qi HY, Qu XJ, Liu J et al: Bufalin induces protective autophagy by Cbl-b regulating mTOR and ERK signaling pathways in gastric cancer cells. *Cell Biol Int*, 2019; 43(1): 33–43
- Gong X, Wang M, Wu Z et al: Pseudolaric acid B induces apoptosis via activation of c-Jun N-terminal kinase and caspase-3 in HeLa cells. *Exp Mol Med*, 2004; 36(6): 551–56
- Guo Z, Guozhang H, Wang H et al: Ampelopsin inhibits human glioma through inducing apoptosis and autophagy dependent on ROS generation and JNK pathway. *Biomed Pharmacother*, 2019; 116: 108524
- Liao CL, Hsu SC, Yu CC et al: The crude extract of Corni Fructus induces apoptotic cell death through reactive oxygen species-modulated pathways in U-2 OS human osteosarcoma cells. *Environ Toxicol*, 2014; 29(9): 1020–31
- He XY, Xiong LL, Xia QJ et al: C<sub>18</sub>H<sub>17</sub>NO<sub>6</sub> and its combination with scutellarin suppress the proliferation and induce the apoptosis of human glioma cells via upregulation of Fas-associated factor 1 expression. *Biomed Res Int*, 2019; 2019: 6821219
- Su ZJ, Liu XY, Zhang JH et al: Neutensin promotes cholangiocarcinoma metastasis via the EGFR/AKT pathway. *Gene*, 2019; 687: 143–50
- Tao H, Tang X, Jin L et al: Synergistic effect of docetaxel combined with cisplatin on inhibiting human osteosarcoma in nude mice. *Biochem Biophys Res Commun*, 2018; 505(2): 372–77
- Zhang Y, Zhao H, Xu W et al: High expression of PQBP1 and low expression of PCK2 are associated with metastasis and recurrence of osteosarcoma and unfavorable survival outcomes of the patients. *J Cancer*, 2019; 10(9): 2091–101
- Hsu MJ, Peng SF, Chueh FS et al: Lupeol suppresses migration and invasion via p38/MAPK and PI3K/Akt signaling pathways in human osteosarcoma U-2 OS cells. *Biosci Biotechnol Biochem*, 2019; 83(9): 1729–39
- Nourmohammadi S, Aung TN, Cui J et al: Effect of compound kushen injection, a natural compound mixture, and its identified chemical components on migration and invasion of colon, brain, and breast cancer cell lines. *Front Oncol*, 2019; 9: 314
- Hung CY, Lee CH, Chiou HL et al: Preruptorin-B inhibits 12-O-tetradecanoylphorbol-13-acetate-induced cell invasion by targeting AKT/NF-κB via matrix metalloproteinase-2/-9 expression in human cervical cancer cell. *Cell Physiol Biochem*, 2019; 52(6): 1255–66
- Gonzalez-Avila G, Sommer B, Mendoza-Posada DA et al: Matrix metalloproteinases participation in the metastatic process and their diagnostic and therapeutic applications in cancer. *Crit Rev Oncol Hematol*, 2019; 137: 57–83
- Singh SK, Mishra MK, Singh R: Hypoxia-inducible factor-1α induces CX3CR1 expression and promotes the epithelial to mesenchymal transition (EMT) in ovarian cancer cells. *J Ovarian Res*, 2019; 12(1): 42
- Xiang Y, Guo Z, Zhu P et al: Traditional Chinese medicine as a cancer treatment: Modern perspectives of ancient but advanced science. *Cancer Med*, 2019; 8(5): 1958–75
- Singh S, Chakrabarti R: Consequences of EMT-driven changes in the immune microenvironment of breast cancer and therapeutic response of cancer cells. *J Clin Med*, 2019; 8(5): 1–20
- Sun Y, Zhou QM, Lu YY et al: Resveratrol inhibits the migration and metastasis of MDA-MB-231 human breast cancer by reversing TGF-β1-induced epithelial-mesenchymal transition. *Molecules*, 2019; 24(6): 1131
- Jiang X, Zhang Z, Song C et al: Glucocalyxin A reverses EMT and TGF-β1-induced EMT by inhibiting TGF-β1/Smad2/3 signaling pathway in osteosarcoma. *Chem Biol Interact*, 2019; 307: 158–66
- Qin G, Luo M, Chen J et al: Reciprocal activation between MMP-8 and TGF-β1 stimulates EMT and malignant progression of hepatocellular carcinoma. *Cancer Lett*, 2016; 374(1): 85–95
- Yang HL, Thiagarajan V, Shen PC et al: Anti-EMT properties of CoQo attributed to PI3K/AKT/NFKB/MMP-9 signaling pathway through ROS-mediated apoptosis. *J Exp Clin Cancer Res*, 2019; 38(1): 186
- Liu J, Ni X, Li Y et al: Downregulation of IQGAP1 inhibits epithelial-mesenchymal transition via the HIF1α/VEGF-A signaling pathway in gastric cancer. *J Cell Biochem*, 2019; 120(9): 15790–99
- XIX Congresso Nazionale S.I.C.O.O.P. Società Italiana Chirurgi Ortopedici Dell'ospedale Privata Accreditata, Capasso L, Florio M, Lilio M et al: Vascular endothelial growth factor expression as a biomarker of prognosis in patients with chondrosarcoma, Ewing's sarcoma and osteosarcoma. *Current concepts. J Biol Regul Homeost Agents*, 2019; 33(2 Suppl.1): 39–43
- Xing XW, Sun YF, Zhao J et al: Tizanidine hydrochloride exhibits a cytotoxic effect on osteosarcoma cells through the PI3K/AKT signaling pathway. *J Int Med Res*, 2019; 47(8): 3792–802
- Ma H, Su R, Feng H et al: Long noncoding RNA UCA1 promotes osteosarcoma metastasis through CREB1-mediated epithelial-mesenchymal transition and activating PI3K/AKT/mTOR pathway. *J Bone Oncol*, 2019; 16: 100228
- Zhang H, Jiang H, Zhang H et al: Anti-tumor efficacy of phellamurin in osteosarcoma cells: Involvement of the PI3K/AKT/mTOR pathway. *Eur J Pharmacol*, 2019; 858: 172477.
- Li ZZ, Wang YL, Yu YH et al: Acridinium bromide inhibits proliferation of osteosarcoma cells through regulation of PI3K/Akt pathway. *Eur Rev Med Pharmacol Sci*, 2019; 23(1): 105–12